

Eurasian Journal of Analytical Chemistry

journal homepage: https://eurasianjournals.com

"Synthesis, Characterization And Biological Activities Of Some Newly Synthesized Macrocyclic Complexes Of Fe(Ii) Metal Ions"

Dr. Sangeeta Gautam¹ & Om Prakash Gurjar^{2*}

 $^{1.2} \text{Department of Science and Technology, Jayoti Vidyapeeth Women's University Jaipur, 303122, Rajasthan, India, <math display="block">\underline{\text{sangeetagautam@jvwu.ac.in}}$

*Corresponding author: Om Prakash Gurjar Email address: omgurjar1512@gmail.com

ARTICLE INFO

Article history: Submission: 27/05/2025 Accepted: 31/05/2025 Publication: 5/06/2025 Available

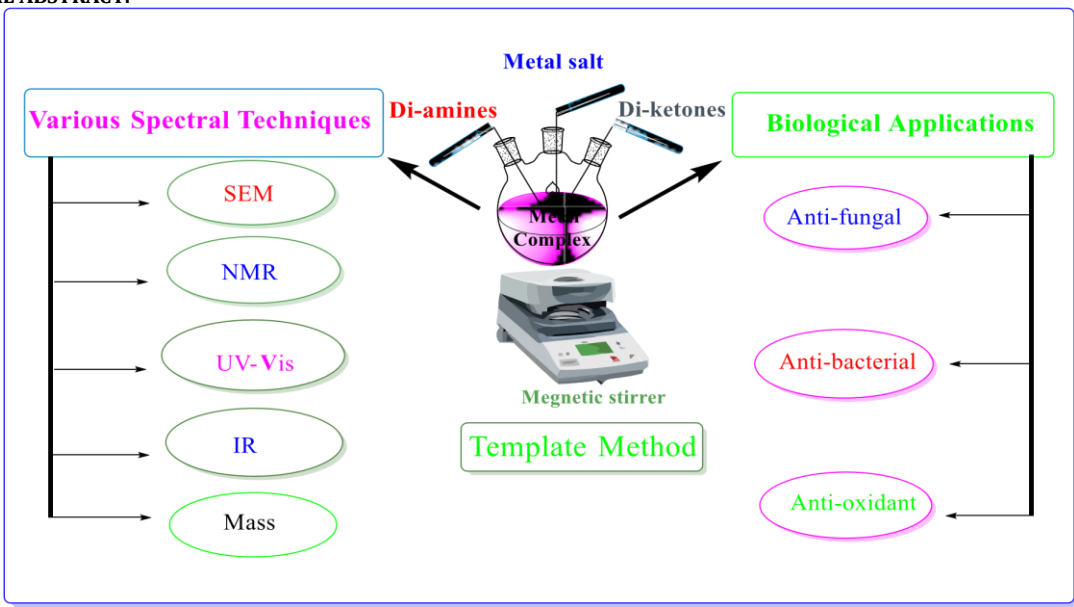
Key words: - Macrocyclic complexes, iron(II), antibacterial, antifungal, antioxidant.

ABSTRACT:

New series of macrocyclic iron complexes, $Fe(C_{30}H_{20}N_8O_2)$ and $Fe(C_{30}H_{18}Cl_2N_8O_2)$, were successfully prepared using a template synthesis method in a methanolic solution. The synthesis of these complexes $involved\ a\ [2+2]\ cyclocondensation\ reaction, where\ diamines, specifically\ 4-aminobenzoic\ hydrazide\ and$ 2-aminobenzhydrazide, were reacted with α-diketones, namely isatin and 5-chloroisatin, in the presence of iron sulphate as a template ion. The physicochemical properties of these complexes were investigated through various methods, including determining their decomposition temperature, conducting conductivity measurements, conducting elemental analyses, and measuring their magnetic moments. It was observed that these complexes exhibited solubility in dimethyl sulphoxide (DMSO). A variety of techniques were employed to analyze the spectra of the synthesized complexes, including scanning electron microscopy (SEM), infrared spectroscopy (IR), nuclear magnetic resonance (NMR) spectroscopy, mass spectrometry, and UV/Visible (UV/Vis) spectroscopy. The antibacterial and antifungal efficacy of all the synthesized complexes was evaluated against bacterial strains such as E. coli and S. aureus, as well as fungal strains like Alternaria alternata and Fusarium solani. This assessment was conducted using the Agar well diffusion method. The antioxidant properties of these complexes were assessed using the DPPH (2,2-diphenyl-1-picrylhydrazyl) method. The results were compared with the standard antioxidant, ascorbic acid, and demonstrated satisfactory antioxidant activity.

2025 Elsevier Ltd. All rights reserved

GRAPHICAL ABSTRACT:



1.0 INTRODUCTION

In recent times, researchers have shown a growing interest in aza macrocycles within the field of coordination chemistry, mainly because of their exceptional characteristics [1–6]. The study of metal macrocyclic chemistry is experiencing rapid growth [7-14]. Currently, the synthesis of well-structured macrocycles incorporating metals represents one of the most captivating and actively researched domains in the field of chemistry [15-18]. The

macrocyclic effect makes macrocyclic ligands more favourable compared to their acyclic counterparts [19]. This preference arises from their higher thermodynamic stability, conformational constraints, the presence of a compact binding site for the metal ion, and the ability to provide a well-structured ligand molecule with minimal entropy and a strong field simultaneously [20]. The structure and reactivity of several notable naturally occurring compounds, well-known for their capability to engage in selective cation complexation, share resemblances with macrocyclic

compounds [21-22]. These macrocyclic complexes play a significant role in various biological activities, including but not limited to antitumor, antidiabetic, antibacterial, anticancer, antifungal, and more [23-30]. The synthesis of macrocyclic complexes can occur through a template condensation process, which serves as a central method in macrocyclic chemistry [31-32]. As a result, the synthesis of macrocyclic compounds often involves the use of the template process [33], with transition metal ions typically serving as templates [34-35]. A considerable number and diversity of transition metal complexes containing novel aza groups have been generated by modifying cavity sizes, donor types, ring substituents, and various other factors [36-40]. Transition metal macrocyclic complexes have garnered significant research interest due to their biocidal effects, which encompass antiviral, anticarcinogenic, antifertility, antibacterial, antifungal properties, and more [41-45]. Iron serves as a critical component in the active sites of various metalloenzymes, including those involved in catalyzing reactions such as hydrogenase and aconitase. Numerous researchers have reported the significance of iron complexes due to their biological, chemical, and catalytical properties [46-47]. Macrocyclic complexes of Fe³⁺/Fe²⁺ exhibit a broad range of redox potentials, making them valuable for various applications related to electron transfer and energy. The redox couple of iron (Fe3+/Fe2+) and (Fe2+/Fe0) has been employed in redox flow batteries as electrolytes [48]. Iron complexes containing amide groups play a crucial role in providing significant structural and functional utility to metallobiomolecules. Examples include iron bleomycin [49-51], nitrile hydratase [52-53], and their involvement in catalytically active oxidation reactions [54-55]. The synthetic chemistry of Fe(II) complexes with ligands containing amide groups [56-58], which can be employed for more efficient oxygenation studies, has received less attention in research compared to the synthesis of Fe(II) complexes with the same ligands [59]. In recent times, iron, particularly in the form of Fe304 nanoparticles, has found diverse applications. These applications include drug delivery systems with drug-release capabilities that respond to pathological environments, as well as supplementary applications in photothermal therapy (PTT) and imaging-guided cancer therapy. Additionally, Fe304 nanoparticles have been used in conjunction with mesoporous silica nanoparticles (MSN) for hormone delivery in response to strong acidic or strong alkaline environments [60]. They have demonstrated ultrafast separation of cationic dyes [61], magnetic responsive controlled release [62], and the functionalization of membrane proteins for binding guest molecules, which can be enriched and then released with the help of an external magnetic field and heating [63]. Iron nanoparticles have also been utilized for responsive payloads in MSNs, taking advantage of the oscillating magnetic field generated by the magnetism-hyperthermia properties of Zn-doped Fe304 nanocrystals, as well as for dye delivery [64]. Furthermore, they have been applied in enzyme-responsive drug release [65]. These versatile iron-based applications span synthetic, biological, and commercial domains, capturing the interest of researchers in this field. In our research, we present the results of the synthesis, physicochemical analysis, and various biological activities of Fe(II) complexes obtained from 4-aminobenzoic hydrazide and 2aminobenzhydrazide in combination with α-diketones, namely isatin and 5-chloroisatin.

2.0 EXPERIMENTAL

2.1 Materials and methods

In the synthesis process, all the chemicals and solvents employed were of pure quality. The ferrous sulphate (FeSO₄·7H₂O) metal salt used in the study was of the Rankem brand, while the ligand precursors, including 5chloroisatin, 2-aminobenzhydrazide, 4-aminobenzoichydrazide, and isatin, were sourced from Sigma Aldrich. The reaction was conducted in a methanolic medium, and the methanol solvent was purified before being utilized.

2.2 Synthesis of the complexes

The formation of all the complexes involved a [2+2] cyclocondensation reaction between either 4-aminobenzoic hydrazide or 2-aminobenzhydrazide and isatin or 5-chloroisatin. This reaction took place in a methanol solvent with ferrous sulphate metal salt serving as a template. For the synthesis of complex (1), a round-bottom flask was used, and 0.4 grams of 2aminobenzhydrazide was dissolved in 15-20 mL of metholic solution. The mixture was then refluxed on a magnetic stirrer. In the synthesis process, the solution of 2-aminobenzhydrazide in methanol was added drop by drop to the previous solution with continuous stirring. Simultaneously, 0.411 grams of isatin was dissolved in 15-20 mL of methanol. To this isatin solution, a methanolic solution of ferrous sulphate (0.11 grams of ferrous sulphate in 15-20 mL of methanol) was also added drop by drop with continuous stirring. The entire mixture was then refluxed for duration of 6-7 hours [66]. Following the refluxing process, the mixture was allowed to cool overnight, during which time it settled down, and a coloured precipitate was formed. The same procedure was followed for the synthesis of complexes (2), (3), and (4), with adjustments made for their respective molar masses. Both the ligands and the metal salt were combined in a [2:2:1] molar ratio, as illustrated in schemes (1) and (2).

2.3 Isolation of the complexes

The colored precipitate of the complexes was separated by filtration using a suction pump, washed thoroughly with methanol several times, and then dried under vacuum. The yield of the complexes ranged between 70% and 80%.

2.4 Characterization and physicochemical properties of the complexes

The synthesized complexes were determined to be soluble in both dimethylformamide (DMF) and dimethyl sulphoxide (DMSO). The produced complexes appeared as dark green, yellow, and light orange-colored solids. Their decomposition temperatures were observed to fall within the range of 230 to 257 °C. The magnetic moments of these complexes were determined to be in the range of 4.81 to 4.90 Bohr magnetons (B.M.) at room temperature. This range suggests the presence of four unpaired electrons in the iron metal ion within the complexes. The presence of the metal in the complex was confirmed with reference to previously reported articles [67]. The scanning electron microscope (SEM) images of the synthesized complexes (1) and (3), as depicted in Fig. 1, revealed a needle-shaped structure for the complexes with an irregular distribution.

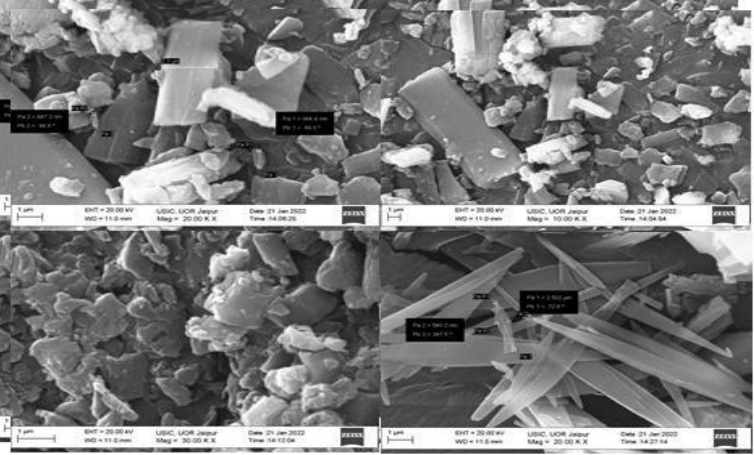


Fig. 1 SEM images of the complexes (1) & (3)

Scheme 1 Synthesis of complexes 1 & 2 derived by the reaction of 2-aminobenzhydrazide with isatin or 5chloroisatin respectively

Scheme: 2 Synthesis of complexes 3 & 4 derived by the reaction of 4-aminobenzoichydrazide with isatin or 5chloroisatin respectively

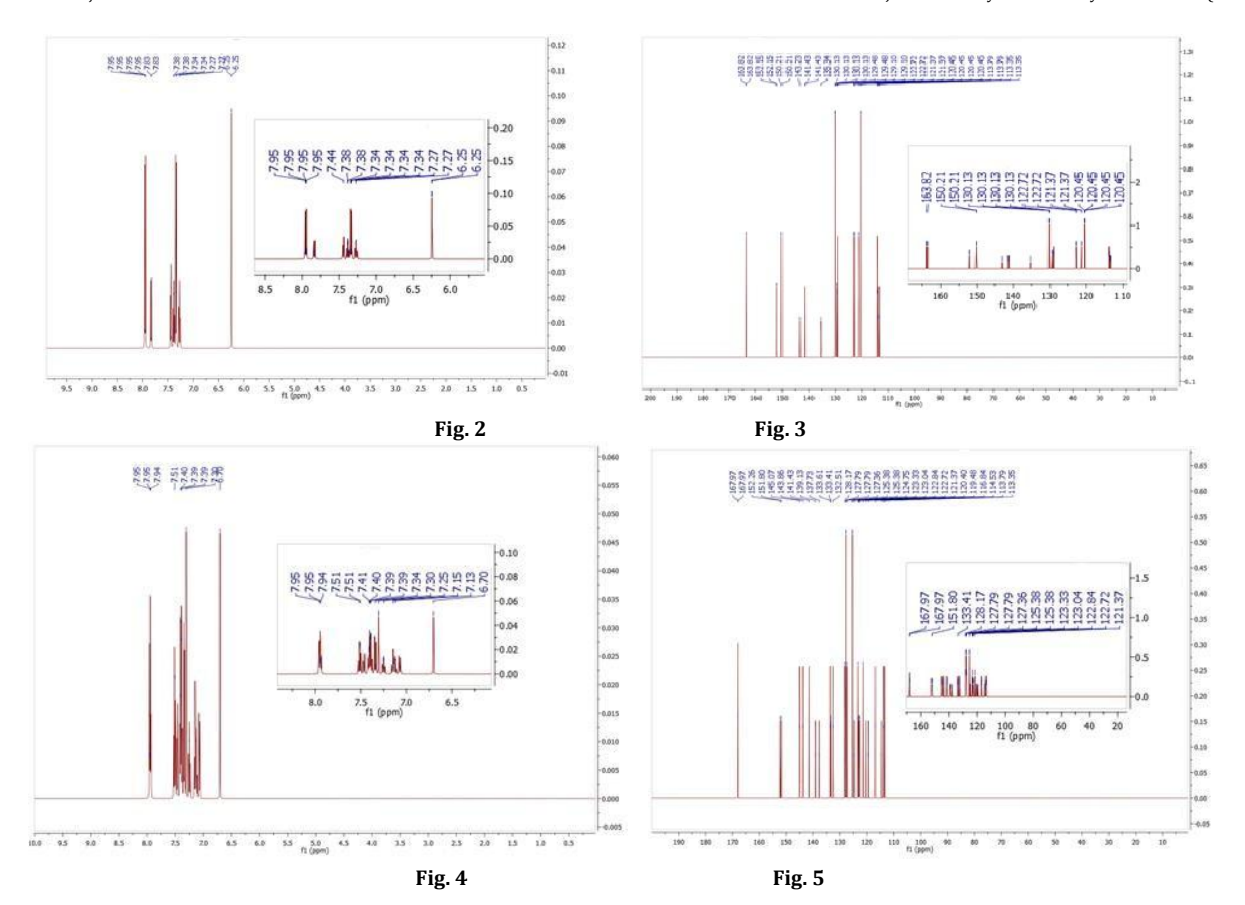
3.0 RESULT AND DISCUSSION

A fresh series of iron complexes with the composition $Fe(C_{30}H_{20}N_8O_2)$ and $Fe(C_{30}H_{18}Cl_2N_8O_2)$ were synthesized as indicated in **schemes 1** and **2** for complexes **1** to **4**. If you have any specific questions or need more information about these complexes or their synthesis, please feel free to ask. All of the compounds were observed to be both soluble and stable in dimethyl sulphoxide (DMSO) and dimethylformamide (DMF), and they exhibited stability in the presence of air. The assumption that complexes were formed was supported by the results obtained from SEM, NMR, UV/Vis, IR, and mass spectrometry analyses.

3.1 NMR spectra

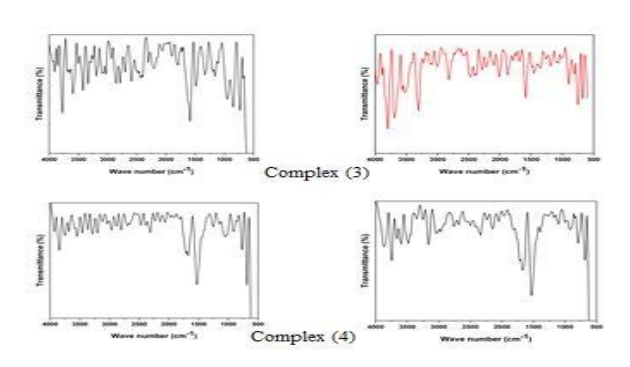
The ¹H NMR and ¹³C NMR spectra of the complexes, which were recorded in a DMSO-d6 solution at room temperature, did not exhibit any signals from the primary amine protons. This suggests that the primary amine groups in the complexes may have undergone coordination with the metal ions, leading to a change in their chemical environment and resulting in the absence of signals in the NMR spectra. The 13C NMR signals provided information about the carbons within the macrocyclic skeleton, while the ¹H NMR spectra revealed the types of protons present. By analyzing the spectral peaks, appropriate positions of the carbons and hydrogens corresponding to the proposed structure were selected. This spectral analysis allowed for a better understanding of the structural features of the synthesized complexes. The ¹H NMR and ¹³C NMR spectra of the $[Fe(C_{30}H_{20}N_8O_2)]SO_4$ complex, as depicted in Fig. 2 and Fig. 3, respectively, support the proposed structural skeleton of Complex-3. These spectra provide evidence for the structural features and composition of the complex, confirming its alignment with the proposed structure. The appearance of two singlet signals at 5.94 ppm in the NMR spectrum suggests the presence of protons connected to the aromatic ring through a -NH- group. These signals provide important information about the chemical structure and connectivity in the compound being analyzed. The

presence of multiple signals in the range of 7.30-7.95 ppm in the NMR spectrum is characteristic of protons attached to aromatic (=CH) groups. These signals correspond to the aromatic regions of the compound's structure and provide information about the chemical environment of these protons. In the ¹³C NMR spectrum, signals within the range of 113.35 to 152.15 ppm are typically classified as carbon atoms in aromatic (=C-) environments. Additionally, signals corresponding to aliphatic carbon atoms in C=N and C=O groups were observed at 150.21 and 163.82 ppm, respectively. These NMR signals help identify the various carbon environments in the compound, which is essential for structural elucidation. The ¹H NMR and ¹³C NMR spectra of **Complex-1**, as displayed in Fig. 4 and Fig. 5, respectively, indicate the presence of specific proton and carbon signals. Two singlet signals at 6.20 ppm are attributed to protons connected to the aromatic ring through the -NH- group. Additionally, multiple signals within the range of 7.19-7.95 ppm are characteristic of protons attached to aromatic (=CH) groups. These spectral features provide valuable information about the structural elements of Complex-1. The appearance of multiple singlet signals in the range of 113.35-151.86 ppm in the 13C NMR spectrum is indicative of carbon atoms within aromatic (=C-) environments. Additionally, the presence of two doublet signals at 125.38 and 127.79 ppm further supports the assignment to aromatic (=C-) carbon atoms. These NMR signals provide valuable structural information about the complex, corroborating the presence of aromatic carbon atoms in its composition. The presence of two singlet signals at $143.59\,\mathrm{ppm}$ and 143.23 ppm in the 13C NMR spectrum can be attributed to carbon atoms in C=N groups. Additionally, the signal at 167.97 ppm is indicative of carbon atoms in C=O groups. Furthermore, a signal at 151.80 ppm corresponds to carbon atoms connected to a -N= group within the aromatic structure. These NMR signals help in the identification of various carbon environments in the complex, which is valuable for understanding its chemical structure [68].



3.2 IR spectra

The absence of two specific bands in the spectra of the complexes, which were present in the spectra of 4aminobenzoichydrazide and 2-aminobenzhydrazide (at 3350 cm-1 and 3390 cm-1 for the former and at 3350 cm¹ and 3385 cm⁻¹ for the latter), indicates that these bands corresponded to the v(NH2) group. The disappearance of these bands in the complexes' spectra suggests a change in the chemical environment of the amino (-NH2) groups, likely due to their involvement in coordination with the metal ions. The presence of a prominent absorption band at 1650 cm-1 is associated with the stretching vibration (v) of the carbonyl group (C=0). This downfield signal suggests the influence of neighbouring electron donor groups on the carbonyl group's chemical environment [69]. This spectral feature can provide insights into the interactions and chemical bonding within the complex. The absence of individual bands corresponding to (>C=O) and (NH₂) groups in the reported range and the presence of a new band at approximately 1590 to 1690 cm⁻¹, attributed to (>C=N) groups, indicate the occurrence of a condensation reaction between the diketone and diamine in all of the complexes. This change in the vibrational modes of the functional groups in the complexes' IR spectra signifies the formation of new chemical bonds and supports the proposed coordination and structural changes in the complexes. The absorption bands within the range of 1400-1588 cm-1 are associated with the various forms of vibrations attributed to the $\upsilon(C=C)$ aromatic stretching in the benzene ring. These spectral features provide information about the structural components and characteristics of the aromatic rings within the complexes [70-71]. The bands observed in the range of 740-785 cm $^{\text{-}1}$ are likely associated with the $\upsilon(\text{C-H})$ outof-plane bending vibrations of the aromatic rings. These vibrations reflect the bending motion of carbon-hydrogen bonds in the aromatic ring structure [72]. The presence of absorption bands in the IR spectra of all the complexes in the ranges of 1408-1440 cm⁻¹, 1290- 1320 cm⁻¹, and 1010-1030 cm⁻¹ indicates that the nitrogen atoms are interacting with and coordinated to the central metal ion. These bands provide evidence of the coordination of nitrogen atoms to the metal core within the complexes [73]. The coordination of the sulphate group with the central metal ion appears to be unidentate, as indicated by the observation that the difference between (vas - vs), in the range of 390-370 cm⁻¹, is greater than 144 cm⁻¹. This difference in wavenumbers is characteristic of unidentate coordination [74]. The IR spectra of the synthesized compounds, Complex-3 and Complex-4, are depicted in Fig. 6. If you have specific questions or need further information regarding these spectra or the compounds, please feel free to ask.



 $\textbf{Fig. 6} \ IR \ spectra \ of the \ [Fe(C_{30}H_{20}N_8O_2)]SO_4 \ and \ [Fe(C_{30}H_{18}Cl_2N_8O_2)]SO_4 \ complexes$

3.3 Mass spectrometry

The mass spectra of the $[Fe(C_{30}H_{20}N_8O_2)]SO_4$ and $[Fe(C_{30}H_{18}Cl_2N_8O_2)]SO_4$ complexes have been recorded and are displayed in Fig. 7 and Fig. 8, respectively. If you have specific questions or need further information about these mass spectra or the complexes, please feel free to ask. The compound $[Fe(C_{30}H_{20}N_8O_2)]SO_4$ displayed a molecular ion peak (M^+) with a mass-to-charge ratio (m/z) of 524.17 in the mass spectrum. This peak represents the intact molecular ion of the compound. The presence of the molecular ion peak $[Fe(C_{30}H_{20}N_8O_2)]SO_4$ at m/z = 524.17 in the mass spectrum confirms the formation of the macrocyclic structure. Additional peaks at m/z = 525.17, 526.18, and so on, may correspond to various fragment ions or isotopic variations of the compound. These additional peaks provide insights into the fragmentation and structure of the complex. The complex [Fe($C_{30}H_{18}Cl_2N_8O_2$)]SO₄ exhibited a molecular ion peak (M+) with a mass-to-charge ratio (m/z) of 592.09 in the mass spectrum. This peak confirms the formation of the macrocyclic structure with the chemical formula [Fe($C_{30}H_{18}Cl_2N_8O_2$)]. The presence of the M+ peak is a key indicator of the intact molecular ion of the compound, supporting its structural identification. The presence of additional peaks at m/z = 592.0901,

 $593.1001,\,594.0902,\,595.0912,\,596.0912,\,$ and so on in the mass spectrum of the complex $[Fe(C_{30}H_{18}Cl_2N_8O_2)]SO_4$ suggests the presence of various fragment ions or isotopic variations of the compound. The intensity of these peaks provides information about the relative stability of the different fragments. This fragmentation pattern can offer valuable insights into the structure and behaviour of the complex during mass spectrometry [75].

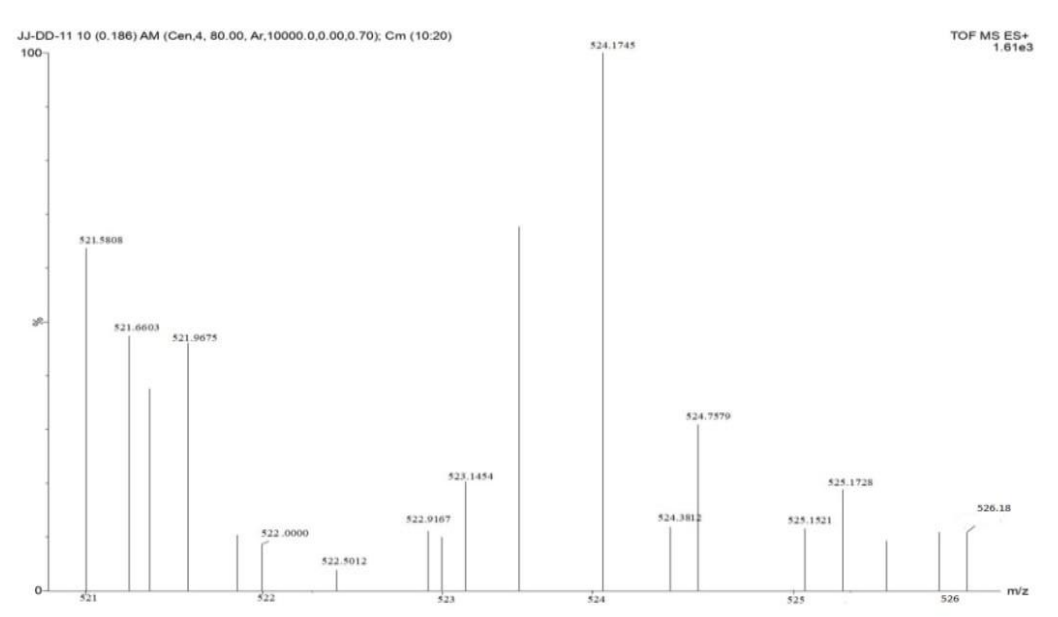


Fig. 7 Mass spectrum of the complex [Fe(C₃₀H₂₀N₈O₂)]SO₄

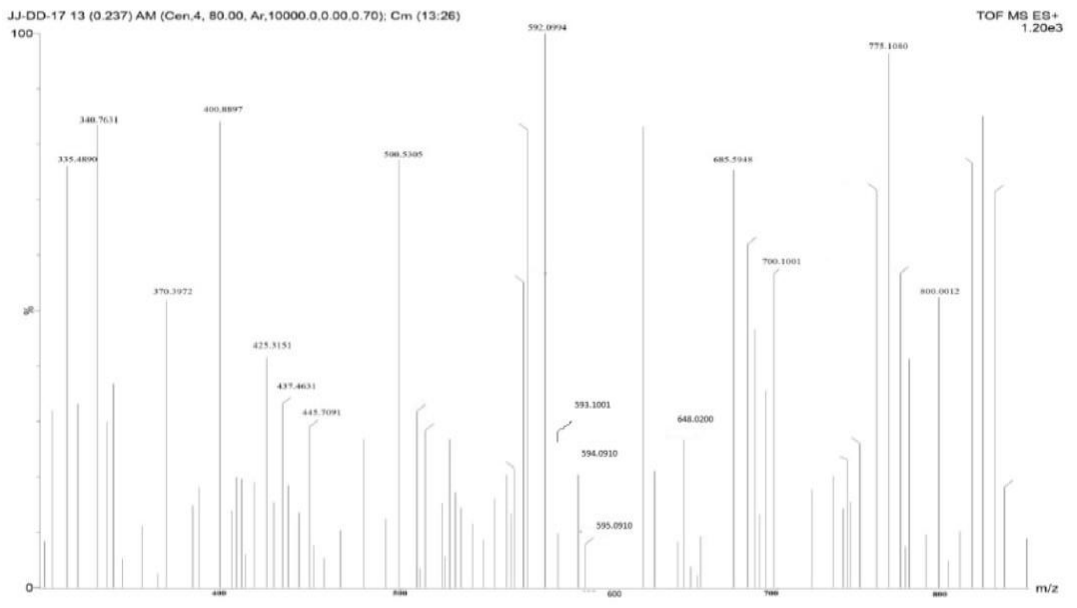


Fig. 8 Mass spectrum of the complex [Fe(C₃₀H₁₈Cl₂N₈O₂)]SO₄

3.4 UV Spectra

The UV-Vis spectra of the respective complexes exhibited both strong and weak peaks in the wavelength range of 254-258 nm and 350-400 nm, respectively. These peaks correspond to different types of electronic transitions. The strong peaks in the range of 254-258 nm are indicative of π to π^* transitions. These transitions are observed at longer wavelengths (254-258 nm) than the typical range of transitions (180-200 nm). The extended conjugation within the complex's structure and the presence of a

polar solvent can lead to these longerwavelength transitions. The weak peaks in the range of 350-400 nm are associated with n to π^* transitions. These transitions involve the movement of electrons from non-bonding (n) orbitals to π^* anti-bonding orbitals. The UV-Vis spectra provide valuable information about the electronic structure and properties of the complexes, including the nature of the electronic transitions and the effects of the complex's structure and the solvent on these transitions. The observed bathochromic shift (shift towards longer wavelengths)

in the UV-Vis spectra can be explained by the impact of increased conjugation within the complex's structure. As conjugation increases, the energy gap between the Highest Occupied Molecular Orbital (HOMO) and the Lowest Unoccupied Molecular Orbital (LUMO) decreases. This reduced energy gap means that less energy is required for electronic transitions, leading to longer-wavelength transitions. The effect of polar solvents on electronic transitions follows the order of $n > \pi^{\ast} > \pi$. In the

presence of a polar solvent, the wavelength of π to π^* transitions tends to increase, resulting in a bathochromic shift, as observed in your spectra. On the other hand, n to π^* transitions decrease in wavelength, showing a hypsochromic shift. These spectral changes illustrate the influence of both conjugation and solvent polarity on the electronic transitions within the complexes, as depicted in Fig. 9.

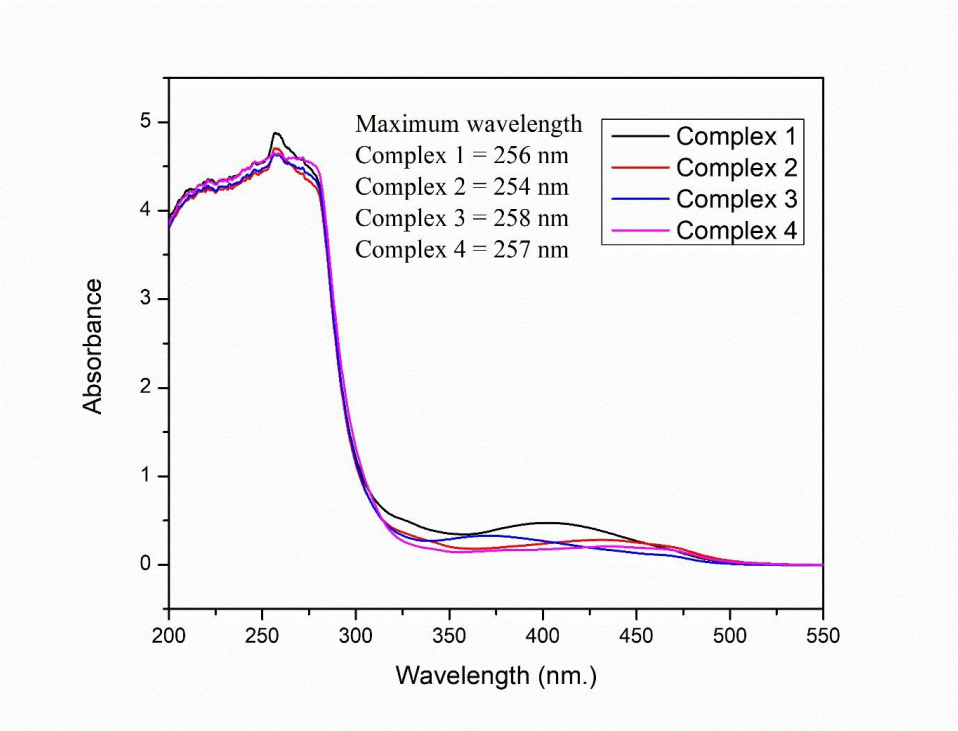


Fig. 9 UV-Vis spectra of the synthesized macrocyclic complexes

4.0 BIOLOGICAL ACTIVITIES

4.1 Antibacterial and Antifungal assay by well diffusion method: -

In the *in-vitro* antibacterial assays, the agar well diffusion method was employed [76]. To prepare the samples for testing, a 10% Dimethyl sulphoxide (DMSO) solution was used as a diluent. Three different concentrations of each drug, specifically 50 mg/mL, 100 mg/mL, and 200 mg/mL, were utilized. For inoculating the test microorganisms, nutrient agar medium was used for the antibacterial assays, while potato dextrose agar (PDA) medium was employed for the antifungal assays. These media were placed in clean petri dishes to facilitate the growth and assessment of the antimicrobial activity of the samples. The procedure involved:

- ➤ Using a spreader to evenly distribute the microbial inoculum on the agar surface, followed by allowing the dish to stand for 30 minutes.
- ➤ Preparing seeded agar plates with 6 mm-diameter wells, including a control well set up at the same distance from the sample wells.

- \triangleright Filling the prearranged wells in the seeded plates with various concentrations of each sample and a standard medication, with a volume of 30 μ l for each.
- Incubating these plates at 37°C for duration of 24 hours.
- Measuring the inhibition zones (IZ) surrounding each prepared well to determine the antifungal and antibacterial spectrum of the test material.

Comparisons were made between the diameter of the inhibitory zone produced by the test sample and the commercially available control antibiotics, which were Cipro (1 mg/mL) for antibacterial testing and Ketoconazole (1 mg/mL) for antifungal testing. These comparisons help assess the relative effectiveness of the test materials in inhibiting the growth of microorganisms in comparison to established antibiotics. The results of the antibacterial assays conducted against *S. aureus* and *E. coli*, as well as the antifungal assays against *Alternaria alternata* and *Fusarium solani*, are provided in **Table 1** and **Fig.10**.

Table-1 Antibacterial and Antifungal activity of complexes

			14010 1	111101000	toriar arra i	mich angar a	ourrie, o.	сотприсле	,				
Sample's Name	Anti-E	Anti-Bacterial Action						Anti-Fungal Action					
	E. coli			S. aureus			Alternaria alternative			Fusarium solani			
	Concentration					Concentration							
	50	100	200	50	100	200	50	100	200	50	100	200	
	IZ	IZ	IZ	IZ	IZ	IZ	IZ	IZ	IZ	IZ	IZ	IZ	
Standard	25	27	32	27	31	36	32	36	41	28	30	34	
Complex 1	NA	2	3	5	8	10	NA	3	6	1	3	8	
Complex 2	2	3	4	6	9	11	8	13	17	NA	2	6	
Complex 3	NA	3	6	4	8	11	NA	2	5	NA	3	5	
Complex 4	5	9	13	3	7	9	7	10	14	5	8	10	

Note: NA= Non active, IZ= Inhibition zone

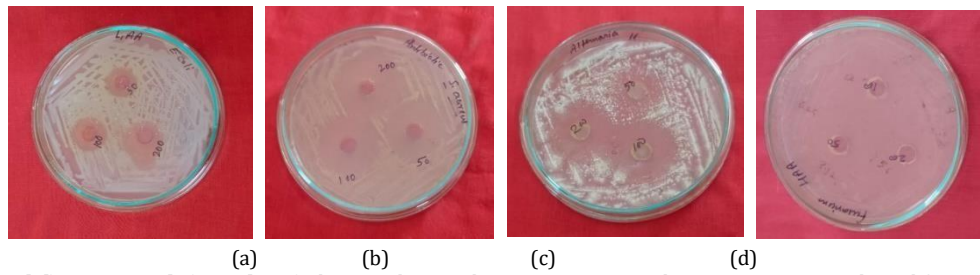


Fig. 10 (a, b, c and d) Figure a & b (complex-2) show antibacterial activity against *E.coli, S. aureus* respectively, and figure c & d (complex-1) show antifungal activity against *Alternaria alternate, Fusarium solani* respectively

4.2 Antioxidant activity: -

The evaluation of the extract's antioxidant characteristics involved performing the DPPH free radical scavenging assay, which utilizes 1,1-diphenyl-2-picryl-hydrazyl (DPPH), as suggested in the method outlined by Alothman $et\ al.$ [77]. A 100 μL portion of compounds at varying concentrations (ranging from 20 to 100 mg/L) was combined with 3.9 mL of a 0.1 mM DPPH solution in methanol. The mixture was then vortexed and left to incubate in the dark for 30 minutes. Optical density (OD) was measured at 515 nm, with methanol serving as the blank for reference.

The percentage of radical scavenging activity is calculated using the formula:

% Radical Scavenging Activity = $[(A0 - Ac) / A0] \times 100$ Where A0 represents the absorbance of the control, and Ac represents the sample's absorbance at the concentration (C). A linear plot was constructed, showing the relationship between concentration and the percentage of inhibition. From this plot, IC50 values were determined. The IC50 value represents the concentration required to inhibit the development of DPPH radicals by 50%, as determined from the inhibition curve. The antioxidant potential of each extract is expressed in terms of IC50, indicating the concentration required to achieve 50% inhibition. The results regarding the antioxidant effects of the complexes can be found in **Table 2** and **Fig. 11**.

Table 2 Antioxidant activity

Name of Compound	Concent	ration(mg,	/L)		Regression Equation	IC50	
	20	40	60	80	100		
Complex 1	17.54	21.05	22.95	24.56	26.6	Y=0.1345x+23.358	198.08
Complex 2	22.22	22.95	26.6	29.38	32.45	Y=0.0861x+27.827	257.52
Complex 3	23.39	25.43	27.63	28.65	31.14	Y=0.1082x+16.051	313.76
Complex 4	29.54	31.66	32.47	34.61	36.67	Y=0.1345x+18.653	233.06
Ascorbic acid	48.09	61.11	70.46	72.8	74.85	Y=0.3261x+45.899	12.57

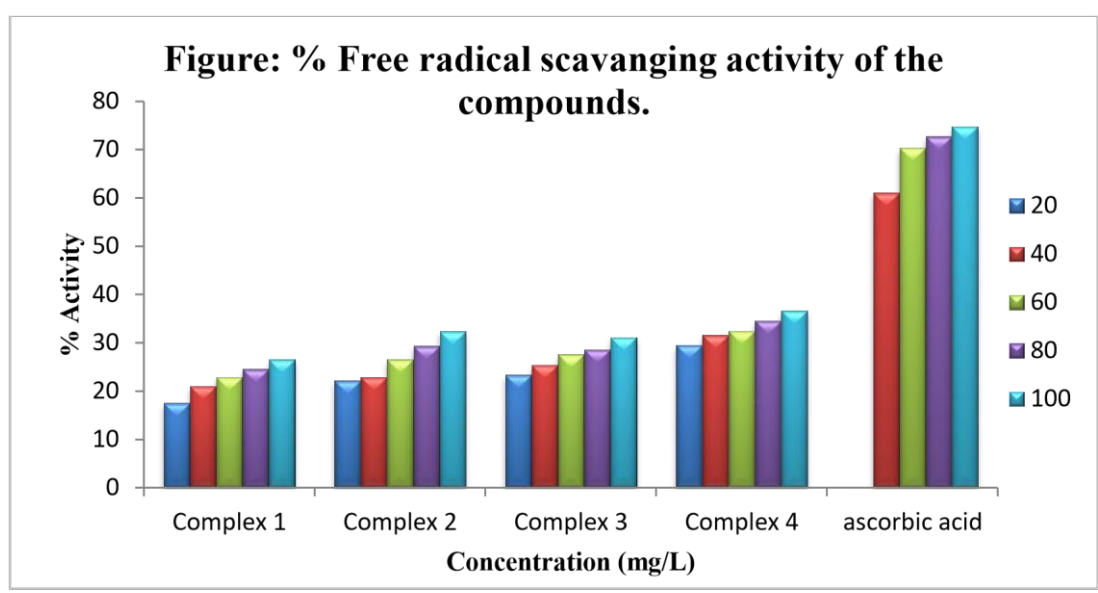


Fig. 11 Comparison of the percentage free radical scavenging activity of the complexes with standard ascorbic acid

5.0 CONCLUSION

Various methods, such as scanning electron microscopy (SEM), nuclear magnetic resonance (NMR), mass spectrometry, infrared spectroscopy (IR), and ultraviolet/visible spectroscopy (UV/Vis), were employed to synthesize and characterize Fe(II) complexes using hexadentate macrocyclic ligands. Complex-4 demonstrated robust antibacterial efficacy against *E. coli*. All the complexes exhibited activity against *S. aureus*, but complex2 and complex-3 displayed particularly satisfactory or notable activity. Complex-2 and complex-4 demonstrated strong antifungal activity against *Alternaria alternate*, while complex-1 and complex-4 exhibited notable antifungal activity against *Fusarium solani*. Complex-2

and **Complex-4** displayed commendable antioxidant activity, although their activity was lower than that of ascorbic acid. Additionally, various properties such as solubility, magnetic moments, and decomposition temperature were also discussed.

ACKNOWLEDGEMENTS

We would like to acknowledge the Department of Science and Technology, Jayoti Vidyapeeth Women's University Jaipur, India, for their valuable contributions to this research in all aspects. We express our gratitude to MNIT (Jaipur) for their assistance with NMR and Mass spectrometry, CU (Haryana) for UV/Vis analysis,

and Biomitra Life Sciences Pvt. Ltd. (Jaipur) for their support in conducting biological activities.

STATEMENT AND DECLARATIONS:

AUTHORS CONTRIBUTIONS:

All of the authors made significant contributions to the preparation of the manuscript titled —SYNTHESIS, CHARACTERIZATION AND BIOLOGICAL ACTIVITIES OF SOME NEWLY SYNTHESIZED

MACROCYCLIC COMPLEXES OF Fe(II) METAL IONS" In this regard, Om Prakash Gurjar completed the experimental section. Moreover, the result and discussion section was researched and written by Om Prakash Gurjar under the supervision of Dr. Sangeeta Gautam. Lastly, all authors reviewed and endorsed the final manuscript.

COMPETING INTERESTS:

The authors do not have any pertinent financial or non-financial interests to declare.

FUNDING: The authors declare that receive financial support from UGC during the preparation of this manuscript.

REFERENCES

- Chandra S, Tyagi M, Agarwal S. Synthesis and characterization of a tetraaza macrocyclic ligand and its cobalt (II), nickel (II) and copper (II) complexes. J. Serbian Chem. Soc. 2010;75(7):935-941. http://dx.doi.org/10.2298/JSC090804069C
- Tyagi M, Chandra S, Choudhary SK. Tetraaza macrocyclic complexes: Synthesis, spectral and antifungal studies. J. Chem. Pharm. Res. 2011;3(1):56-63.
- 3. Khatun M, Ghorai P, Mandal J, Chowdhury SG, Karmakar P, Blasco S, Espana EG, Amrita Saha. ACS Omega. 2023;8(8):7479-7491 DOI: 10.1021/acsomega.2c06549
- Chandra S, Qanungo K, Sharma SK. New hexadentate macrocyclic ligand and their copper (II) and nickel (II) complexes: spectral, magnetic, electrochemical, thermal, molecular modeling and antimicrobial studies. Spectrochimica Acta Part A: Molecular and Biomolecular Spectroscopy.

 2012;94:312-317. https://doi.org/10.1016/j.saa.2011.12.028
- Nirmala G, Rahiman AK, Sreedaran S, Jegadeesh R, Raaman N, Narayanan V. New 14-membered transdi-substituted _teta'macrocycles and their copper (II) and nickel (II) complexes: Spectral, magnetic, electrochemical, crystal structure, catalytic and antimicrobial studies. J. Mol. Struct. 2011;989(1-3):91100. Doi:10.1016/j.molstruc.2011.0101
- Kanaoujiya R, Singh D, Minocha T, Yadav SK, Srivastava S. Synthesis, characterization of ruthenium (III) macrocyclic complexes of 1, 4, 8, 11-tetraazacyclotetradecane (cyclam) and in vitro assessment of anti-cancer activity. Materials Today: Proceedings. 2022; 65:3143-3149.DOI:10.1016/j.matpr.2022.05.354
- 7. Ilhan S, Temel H. Synthesis and characterization of a new macrocyclic Schiff base derived from 2, 6diaminopyridine and 1, 10-bis (2-formylphenyl)-1, 4, 7, 10-tetraoxadecane and its Cu (II), Ni (II), Pb (II), Co (III) and La (III) complexes. Transit. Met. Chem. 2007;32:1039-1046. https://doi.org/10.1007/s11243007-0276-5
- 8. Aly AA, Abdallah EM, Ahmed SA, Rabee MM, Brase S. Transition Metal Complexes of Thiosemicarbazides, Thiocarbohydrazides, and Their corresponding Carbazones with Cu(I), Cu(II), Co(II), Ni(II), Pd(II), and Ag(I)—A Review.

 Molecules. 2023;28:1808. https://doi.org/10.3390/molecules28041808 S
- Ali V, Singh P, Jain V, Tripathi J. Saudi Chem. Soc. 2019;23:52–60 https://doi.org/10.1016/j.jscs.2018.04.005 & Singh P, Tripathi V. IJC-A. . 2020;59A(06):752-759.
- 10. Khalid S, Sumrra SH, Chohan ZH. Sains Malaysiana. 2020;49(8):1891-1904. http://dx.doi.org/10.17576/jsm-2020-4908-11
- 11. Li J, Guo L, Huo H. Preparation of nickel catalysts bearing Schiff base macrocycles and their performance in ethylene

- oligomerization. Transit Met Chem. 2023 https://doi.org/10.1007/s11243-02300527-w
- Fierro CM, Smith PD, Light ME. Polyhedron. 2023; 230. https://doi.org/10.1016/j.poly.2022.116222
- Schuman A.J, Raghavan A, Banziger SD, Song Y, Hu ZB, Mash BL, Williams AL, Ren T. Macrocyclic Chromium (III) Catecholate Complexes. Inorg. Chem. 2021;60(7):4447-4455.
- **14.** Kostova I. Inorganics. 2023;11(2):56. https://doi.org/10.3390/inorganics11020056
- 15. Chandra S, Gupta LK, Agrawal S. Modern spectroscopic and biological approach in the characterization of a novel 14-membered [N 4] macrocyclic ligand and its transition metal complexes. Transit. Met. Chem. 2007;32:240-245. https://doi.org/10.1007/s11243-006-0155-5
- 16. Singh DP, Kumar K, Dhiman SS, Sharma J. Antibacterial and antifungal studies of macrocyclic complexes of trivalent transition metal ions with their spectroscopic approach. J. Enzyme Inhib. Med. Chem. 2010;25(1):21-28. https://doi.org/10.3109/14756360902932750
- 17. Rathi P, Singh DP, Surain P. Synthesis, characterization, powder XRD and antimicrobial-antioxidant activity evaluation of trivalent transition metal macrocyclic complexes. C R Chim. 2015;18(4):430-437. https://doi.org/10.1016/j.crci.2014.08.002
- **18.** Lash TD. Molecules. 2023;28(3):1496. https://doi.org/10.3390/molecules28031496
- 19. Cabbiness DK, Margerum DW. Macrocyclic effect on the stability of copper (II) tetramine complexes. J. Am. Chem. Soc. 1969;91(23):6540-6541. DOI: 10.1021/Ja01051A091
- 20. Fabbrizzi L, Paoletti P, Clay RM. Microcalorimetric determination of the enthalpy of a slow reaction: destruction with cyanide of the macrocyclic (1, 4, 8, 11-tetraazacyclotetradecane) nickel (II) ion. Inorg. Chem. 1978;17(4):1042-1046. https://doi.org/10.1021/ic50182a048
- Lindoy LF. Heavy Metal Chemistry of Mixed Donor Macrocyclic Ligands: Strategies for Obtaining Metal Ion Recognition. J Incl Phenom Macrocycl Chem. 1990;171-183.
- Chandra S, Qanungo K, Sharma SK. New hexadentate macrocyclic ligand and their copper (II) and nickel (II) complexes: spectral, magnetic, electrochemical, thermal, molecular modeling and antimicrobial studies. Spectrochim. Acta A Mol. Biomol. Spectrosc. 2012;94:312-317. Doi: 10.1016/j.saa.2011.12.028
- 23. Nath R, Pathania S, Grover G, Akhtar MJ. J. Mol. Struct. 2020. https://doi.org/10.1016/j.molstruc.2020.128900
- 24. Mishra P, Sethi P, Kumari A. Emerging applications and hostguest chemistry of synthetic macrocycles, Res. J. Chem. Environ. 2022;26(7):153-157. DOI:10.25303/2607rjce153167
- 25. Lahari K, Sundararajan R. J. Chem. Sci. 2020;132:94. https://doi.org/10.1007/s12039-017-1398-8
- Yang J, Dai D, Cai Z, Liu YQ, Qin JC, Wang Y, Yang YW. Acta Biomater. 2021;134:664–73. https://doi.org/10.1016/j.actbio.2021.07.050.
- 27. Liu H, Yang J, Yan X, Li C, Elsabahy M, Yang YW, Gao HA. J. Mater. Chem. B. 2021;9:9594–9605. DOI: 10.1039/d1tb02134f
- 28. Dai D, Yang J, Yang YW. Chem. Eur. J. 2022. DOI: 10.1002/chem.202103185 (Invited Contribution).
- Dileepan AGB, Prakash TD, Kumar AG, Rajam PS, Dhayabaran VV, Rajaram RJ. Photochem. Photobiol. BBiol. 2018. Doi:10.1016/j.jphotobiol.2018.04.029
- Bugalia S, Dhayal Y, Sachdeva H, Kumari S, Atal K, Phageria U, Saini P, Gurjar OP. Review on Isatin- A Remarkable Scaffold for Designing Potential Therapeutic Complexes and Its Macrocyclic Complexes with Transition Metals. JIOPM. 2023. https://doi.org/10.1007/s10904-023-02666-0
- 31. Curtis NF. Macrocyclic coordination compounds formed by condensation of metal-amine complexes with aliphatic carbonyl compounds. Coord. Chem. Rev. 1968;3(1):3-47. https://doi.org/10.1016/S00108545(00)80104-6
- 32. Shakir M, Bano N, Rauf MA, Owais M. J. Chem. Sci. 2017;129(12):1905–1920. https://doi.org/10.1007/s12039-017-1398-8
- 33. Niasari MS, Davar F. In situ one-pot template synthesis (IOPTS) and characterization of copper (II) complexes of 14-membered hexaaza macrocyclic ligand —3, 10-dialkyl-

- dibenzo-1, 3, 5, 8, 10, 12hexaazacyclotetradecane||. Inorg. Chem. Commun. 2006; 9(2):175-179. D0I:10.1016/j.inoche.2005.10.028
- 34. Prasad RN, Mathur M, Upadhyay A. Synthesis and spectroscopic studies of Cr (III), Fe (III) and Co (II) complexes of hexaazamacrocycles. J. Indian Chem. Soc. 2007;84(12):1202-1204.
- 35. Kamboj M, Singh DP, Singh AK, Chaturvedi D. Molecular modeling, in-silico docking and antibacterial studies of novel template wangled macrocyclic complexes involving isatin moiety. J. Mol. Struct. 2020;1207:127602. DOI:10.1016/j.molstruc.2019.127602
- 36. Chandra S, Qanungo K, Sharma SK. New hexadentate macrocyclic ligand and their copper (II) and nickel (II) complexes: spectral, magnetic, electrochemical, thermal, molecular modeling and antimicrobial studies. Spectrochim. Acta A Mol. Biomol. Spectrosc. 2012;94:312-317. Doi: 10.1016/j.saa.2011.12.028
- 37. Martin JG, Wei RM, Cummings SC. Copper (II) complexes with 13-membered macrocyclic ligands derived from triethylenetetramine and acetylacetone. Inorg. Chem. 1972;11(3):475-479.
- 38. Holtman MS, Cummings SC. Macrocyclic nickel (II) complexes with new, dimethyl-substituted 13-and 14-membered tetraaza ligands. Inorg. Chem. 1976;15(3):660-665.
- 39. Roberts GW, Cummings SC, Cunningham JA. Synthesis and characterization of low-spin cobalt (II) complexes with macrocyclic tetraaza ligands. The crystal structure of [Co ([14] dieneN4). cntdot. H_2O (PF6) 2. Inorg. Chem. 1976;15(10):2503-2510.
- 40. Coltrain BK, Jackels SC. Coordination chemistry of a copper (II) tetraimine macrocycle: four-, five-, and six-coordinate derivatives and reduction transmetalation to the zinc (II) complex. Inorg. Chem. 1981;20(7):2032-2039. https://doi.org/10.1021/ic50221a021
- 41. Chandra S, Pundir M. Spectroscopic characterization of chromium (III), manganese (II) and nickel (II) complexes with a nitrogen donor tetradentate, 12-membered azamacrocyclic ligand. Spectrochim. Acta A Mol. Biomol. Spectrosc. 2008;69(1):1-7.
- 42. Prasad RN, Upadhyay A. Chromium (III), iron (III) and cobalt (II) complexes of 14-and 16-membered tetraazamacrocycles. J. Indian Chem. Soc. 2006;83(9):857-860.
- 43. Chandra S, Gupta R, Gupta N, Bawa SS. Biologically relevant macrocyclic complexes of copper spectral, magnetic, thermal and antibacterial approach. Transit. Met. Chem. 2006;31(2):147-151.
- 44. Chandra S, Gupta LK, Agrawal S. Synthesis spectroscopic and biological approach in the characterization of novel [N 4] macrocyclic ligand and its transition metal complexes. Transit. Met. Chem. 2007;32:558563.
- 45. Gammal OAE, Brashy SAE, El-Reash GMAE. Macrocyclic Cr3+, Mn2+ and Fe3+ complexes of a mimic SOD moiety: Design, structural aspects, DFT, XRD, optical properties and biological activity. Appl. Organomet. Chem. 2020;34(4):5456. DOI:10.1002/aoc.5456
- Habtemariam AB, Sibhatu AK, Weldegebrieal GK, Zelekew OA, Tekletsadik BT. Lett. Appl. NanoBioScience, 9, 808(2020). https://doi.org/10.33263/LIANBS91.808813.
- 47. Subhanandaraj TT, Raghavan KT, Narayanan R. **9**, 988(2020). https://doi.org/10.33263/LIANBS92.988994.
- 48. Hruska LW and Savinell R F. J. Electrochem. Soc. 128 18 (1981)
- 49. Richard M, Burger, American chemical society, chem. Rev., **98(3)**, 1153(1998). S0009-2665(96)00438-4 CCC.
- 50. Sidney M, Hecht. The chemistry of activated Bleomycin, American chemical society **19**, 383(1986). 0001-4842/86/0119-0383.
- Joanne S, Kozarich JW, Wei W and Dana E. Vanderwall, Bleomycins, Aerican chemical society, 29, 322(1996). S0001-4842(95)00133-6CCC.
- 52. Huang W, Jia J, Cummings J, Nelson M, Schneider G and Lindquist Y. Crystal structure of nitrile hydrate, **5(5)**, 661(1997). http://biomednet.com/elecref/0969212600500691.
- 53. Novel non-heme Iron center of nitrile hydratase with a claw setting of oxygen atoms, Nature structured biological, **5(5)**, 347(1998).

- 54. Collins TJ. J. Am. Chem. Soc., 27, 279(1994).
- 55. Nguyen C, Guajardo RJ and Mascharak PK. J. Am. Chem. Soc., **35**, 6273(1996).
- Brown SJ, Olmstead MM and Mascharak PK. J. Am. Chem. Soc., 29, 3229(1990).
- 57. Umezawa H, Takita T, Sugiura Y, Otsuko M, Kobayashi S and Ohno M. Tetrahedron, **40(3)**, 501(1984).
- 58. Zhu S, Brennessel WW, Harrison RG, Que LJ. Inorganic chim. Acta-337, 32(2002).
- 59. Marlin DS and Mascharak PK. RSC, 29, 69(2000).
- Li T, Fang Q, Xi X, Chen Y and Liu F. J. Mater. Chem. C, 7, 586(2019). DOI: 10.1039/c8ta08829b.
- 61. Zhang H, Wu JR, Wang X, Li XS, Wu MX, Liang F and Yang YW. Dyes and Pigments **162**, 512(2019). https://doi.org/10.1016/j.dyepig.2018.10.061.
- Zhou J, Chen M and Diao G. J. Am. Chem. I soc., XXXX, (XXX), XXX-XXX (2014). dx.doi.org/10.1021/am5057147.
- 63. Zhu H, Liu J, Shi B, Wang H, Mao Z, Shan T and Huang F. Mater. Chem. Front, **2**, 1475(2018).
- 64. Thomas CR, Ferris DP, Lee JH, Choi E, Cho MH, Kim ES, Stoddart JF, Shin JS, Cheon J and Zink JI. J. Am. Chem. Soc., 132, 10623(2010).
- Qiao H, Jia J, Shen H, Zhao S, Chen E, Chen W, Di B and Hu C. Enzyme Adv. Healthcare Mater, 1900174(1 of 10) (2019). DOI:10.1002/adhm.201900174
- 66. Zafar H, Kareem A, Sherwani A, Mohammad O, Khan TA. Synthesis, characterization and biological studies of homo and hetero-binuclear 13-membered pentaaza bis (macrocyclic) complexes. J. Mol. Struct. 2015;1079:337–346. http://dx.doi.org/10.1016/j.molstruc.2014.08.036
- 67. Drahos B, Antal P, Salitros I, Herchel R. Magnetic properties of Fe(II) complexes of cyclam derivative with one p-aminobenzyl pendant arm. Metals 2020, 10, 366; https://doi.org/10.3390/met10030366
- 68. Zafar H, Kareem A, Sherwani A, Mohammad O, Khan TA. Synthesis, characterization and biological studies of homo and hetero-binuclear 13-membered pentaaza bis (macrocyclic) complexes. J. Mol. Struct. 2015;1079:337–346. http://dx.doi.org/10.1016/j.molstruc.2014.08.036
- 69. Singh DP, Kumar R, Singh J. Antibacterial activity and spectral studies of trivalent chromium, manganese, iron macrocyclic complexes derived from oxalyldihydrazide and glyoxal. J Enzyme Inhib Med Chem. 2009;24(3):883-889.
- 70. Prasad RN, Mathur M, Upadhyay A. Synthesis and spectroscopic studies of Cr (III), Fe (III) and Co (II) complexes of hexaazamacrocycles. J. Indian Chem. Soc. 2007;84(12):1202-1204.
- 71. Costamagna J, Ferraudi G, Villagran M, Wolcan E. Ligand luminescence and photoinduced charge separation in bis (naphthalene) substituted fourteen-membered tetraazamacrocyclic complexes of Cu II and Ni II. J. Chem. Soc., Dalton Trans. 2000;(15):2631-2637. https://doi.org/10.1039/B002829K
- 72. Singh DP, Shishodia N, Yadav BP, Rana VB. Trivalent transition metal ion directed macrocycles. J. Indian Chem. Soc. 2004; 81(4):287-290.
- 73. Chandra S, Gupta LK. Electronic, EPR, magnetic and mass spectral studies of mono and homo-binuclear Co (II) and Cu (II) complexes with a novel macrocyclic ligand. Spectrochim. Acta A Mol. Biomol. Spectrosc. 2005;62(4-5):1102-1106. Doi: 10.1016/j.saa.2005.04.007
- 74. Nakamoto K. Infrared and Raman spectra of inorganic and coordination compounds, part B: applications in coordination, organometallic, and bioinorganic chemistry. John Wiley & Sons. 2009.
- Singh DP, Kumar K, Dhiman SS, Sharma J. Biologically active macrocyclic complexes derived from diaminonaphthalene and glyoxal: Template synthesis and spectroscopic approach.
 J. Enzyme Inhib. Med. 2009;24(3):795–803. DOI: 10.1080/14756360802397179
- Pérez C, Anesini C. Antibacterial activity of alimentary plants against Staphylococcus aureus growth. Am. J. Chinese Med. 1994; 22(02):169-174.
- 77. Alothman M, Bhat R, Karim AA. Antioxidant capacity and phenolic content of selected tropical fruits from Malaysia, extracted with different solvents. Food Chem. 2009;115(3):785-788.